A. Experimental setup and procedure

Figure 1S shows a block diagram of the corresponding experimental setup. The main functional units are a solid-state pulsed NMR spectrometer for detection, an electromagnet for field-cycling (the external magnetic field is switched adiabatically within approximately 10 s) between the levels for polarization and detection, a pulsed light source and a high power channel for radiofrequency (rf) irradiation. For temperature variation a conventional flow cryostat (Oxford) is used. All components are connected to a computer system for on-line data processing and process control.

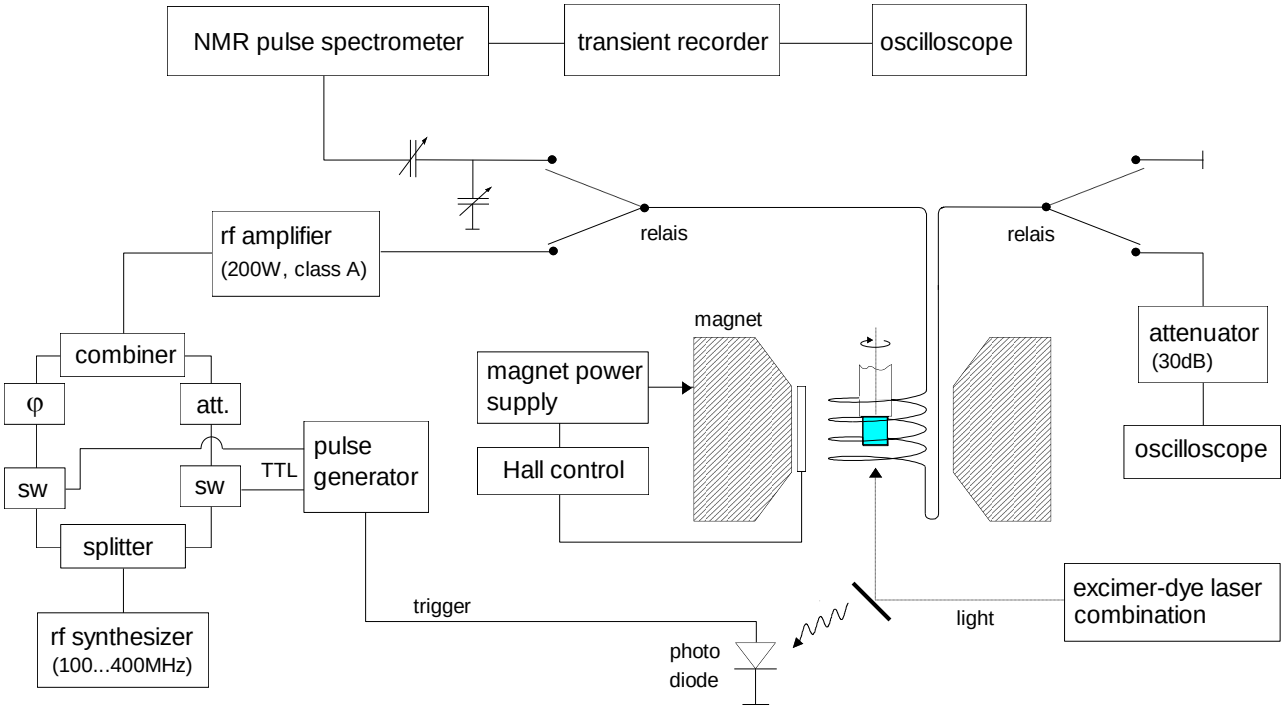

Figure 1S: Block diagram of the ONP spectrometer. See text for discussion.

NMR detection is performed at a fixed detection field of $B_{det} = 705$ mT, corresponding to a proton Zeeman frequency of 30 MHz. As the observable in our experiments is always the magnitude of the final proton polarization, high accuracy in measuring the initial value of the NMR signal in the time domain is essential. This is achieved by applying a pulse sequence, similar to those known from pulsed spin-lock experiments, which increases sensitivity by about an order of magnitude with respect to standard Free Induction Decay (FID) detection. The comparatively low detection frequency was chosen to permit the use of an electromagnet, a Hall controller, and a standard power supply for the necessary field switching. The inhomogeneity across the sample volume is smaller than 50 ppm. The sign of the NMR signal was chosen by adjusting the reference phase in such a way, that the Boltzmann signal of a water sample yields a positive signal.

The sample is situated inside a single coil which can be connected *via* two high-power rf-relays either narrow banded to the NMR detection branch or broad banded to the rf-irradiation branch. In order to allow precise orientation, the sample is attached to a sample holder which can be rotated about an axis perpendicular to the external magnet field. Pulsed light irradiation is performed with an excimer-dye laser combination. The flash profile has approximately Gaussian shape and a pulse length of 15 ns; the maximum repetition rate is around 50 Hz. The wavelength was chosen by optimizing the proton polarization. This optimum is obtained at a wavelength of 550 nm for pentacene/naphthalene (dye: coumarin 153) and at 386 nm for acridine/fluorene (dye: BiBuQ). The pulse energy is about 10 mJ.

phase, followed by a time interval where no rf-fields are applied. For detecting the influence of this free evolution period, the pulse sequence has to be terminated with a fixed detection pulse sequence.

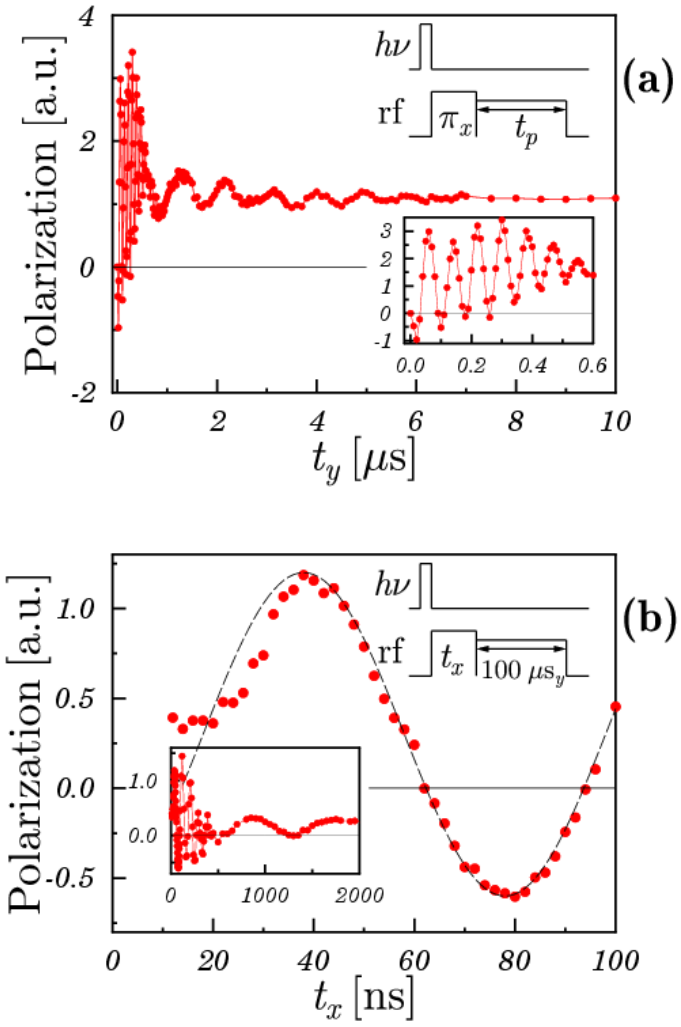

Figure 2S. Polarization obtained using two-pulse sequences with $\varphi = \frac{\pi}{2}$ phase shift. a) $\pi_x - t_y$, b) $t_x - 100$ µs. (System Pe-d_{14}/Na-h_8, $\frac{\omega_{rf}}{2\pi} = 230$ MHz= $\frac{\omega_0}{2\pi}$, $\frac{\omega_n}{2\pi} = 1.2$ MHz, $T = 250$ K).

A delay time can be incorporated within the pulse sequences discussed so far in three different ways. **Figure 3S** shows the result of a variation of a delay time between two pulses without phase shift. In this particular experiment all four combinations of $\frac{\pi}{2}$ and π pulses where applied off-resonant at $\Delta\omega = \sigma_{EPR}$. The sequences, which start with a $\frac{\pi}{2}$ pulse show mainly a fast decay of the signal within the first 100 ns. In addition, a strongly damped oscillation with a frequency which corresponds approximately to $\Delta\omega$ can be observed in this case (see **Figure 3Sa**, $\frac{\pi}{2} - \tau - \pi$). No fast frequency components corresponding to the nutation frequency of $\sqrt{2} \cdot \frac{\omega_1}{2\pi} = 11$ MHz is observed.

In contrast, sequences starting with a π pulse show strong oscillations, with a frequency, which corresponds to the precession frequency $\omega_{pre} = \omega_n$. The amplitude of these oscillations depends on the second pulse and is twice as strong for a terminating π pulse than for a $\frac{\pi}{2}$ pulse.

For irradiation on resonance ($\Delta\omega = 0$) **Figure 4S** shows a variation of a delay time in a $\left(\frac{\pi}{2}\right)_x - \left(\frac{\pi}{2}\right)_y - \tau - t_y$. The experiments were carried out for a fixed value of ω_{rf} above and below the level-crossing field B_{LC}. The absolute value of the achieved proton polarization is the same in both cases. Only the sign of the signal is

opposite, which reflects directly the different sign of the electron spin polarization on both sides of the level crossing region. Both curves show oscillations with a frequency of 1.3 MHz (∘) and 2.0 MHz, respectively. The differences in these frequencies reflect directly the differences in the external magnetic field B_{pol}. Only this precession frequency, but no fast frequency component corresponding to the nutation frequency of $\sqrt{2} \cdot \omega_{1x} = 21$ MHz or $\sqrt{2} \cdot \omega_{1y} = 15$ MHz can be observed.

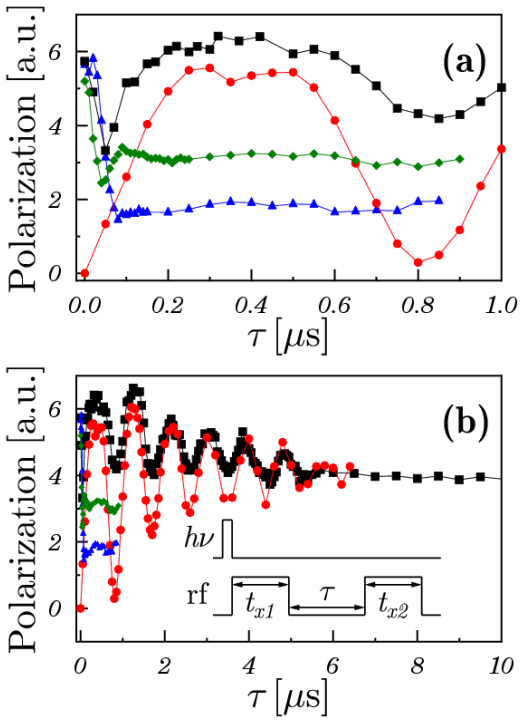

Figure 3S. Variation of a delay time τ (no rf) without phase shift a) on a time scale up to 1 µs and b) on the longer time scale up to 10 µs. The inset in b) shows the applied pulse sequence. The sequence is π-τ-$\frac{\pi}{2}$ (black squares); π-τ-π (red circles); $\frac{\pi}{2}$-τ-π (green diamonds); $\frac{\pi}{2}$-τ-$\frac{\pi}{2}$ (blue triangles). (System Pe-d_{14}/Na-h_8, $\frac{\omega_{rf}}{2\pi} = 230$ MHz= $\frac{\omega_0}{2\pi} + \frac{\sigma_{EPR}}{2\pi}$, $\sqrt{2} \cdot \frac{\omega_1}{2\pi} = 11$ MHz, $\frac{\omega_n}{2\pi} = 1.2$ MHz, $T = 250$ K).

In **Figure 5S** the variation of the delay time τ (no rf) within a $t_x - \tau - t_y$ sequence is shown. The signal shows a fast decay within the first 100 ns, modulated in case of $t_y \mathrel{\widehat{=}} \frac{\pi}{2}$ with a strongly damped oscillation whose frequency is approximately given by σ_{EPR}. On the longer time scale an oscillation with a frequency of 2.0 MHz can be observed, which is more pronounced for a short y-pulse than for a long y-pulse. No frequency components corresponding to $\sqrt{2} \cdot \frac{\omega_{1x,y}}{2\pi} = 12$ MHz can be observed.

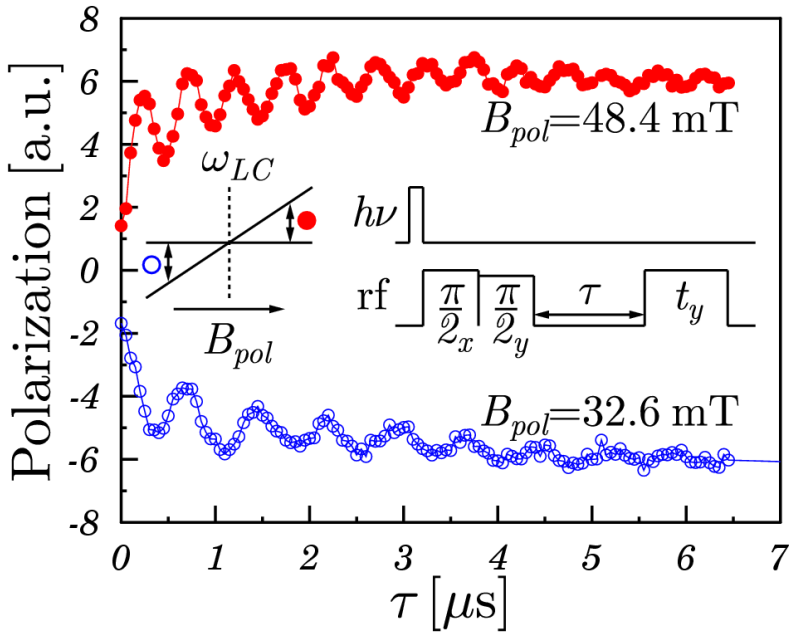

Figure 4S. Variation of a delay time τ (no rf) in a $\left(\frac{\pi}{2}\right)_x - \left(\frac{\pi}{2}\right)_y - \tau - t_y$ sequence with t_y=1.5 μs. The measurements were performed in different polarization fields B_{pol} below (open circles) and above (full circles) the level crossing field B_{LC}. The left inset shows the energy levels of the two coupled triplet sub-levels and the right inset shows the applied pulse sequence. (System Ac-d_9/Fl-d_8h_2, $\frac{\omega_{rf}}{2\pi} = 171$ MHz$= \frac{\omega_0}{2\pi}$, $\sqrt{2} \cdot \frac{\omega_{1x}}{2\pi} =$ 21 MHz, $\sqrt{2} \cdot \frac{\omega_{1y}}{2\pi} = 15$ MHz, $\frac{\omega_n}{2\pi} = 1.34$ (open circles), resp. 2.0 MHz (full circles), $T = 300$ K).

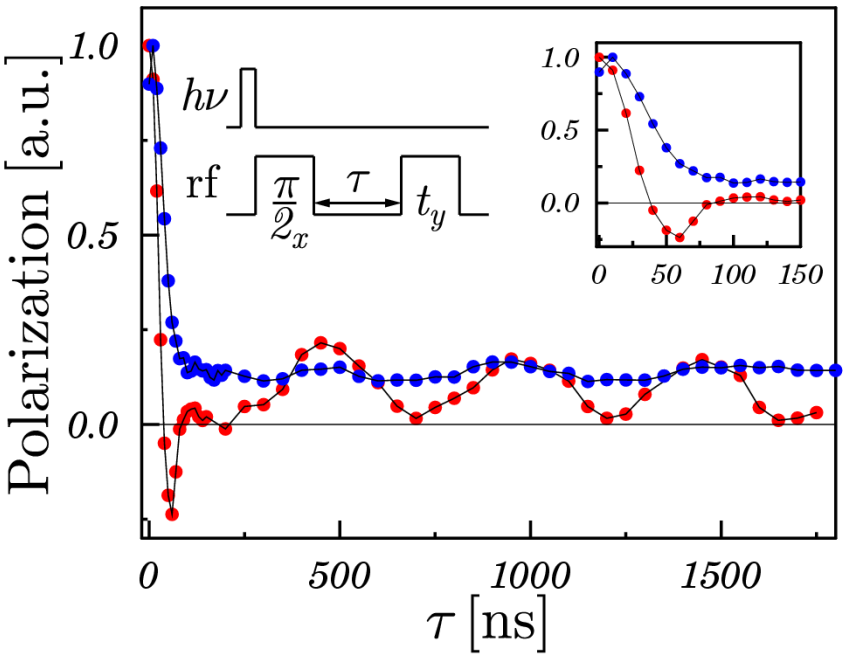

Figure 5S. Variation of a delay time τ (no rf) in a $\left(\frac{\pi}{2}\right)_x - \tau - t_y$ sequence. The inset shows the applied pulse sequence. Here red circles correspond to a $\frac{\pi}{2}$-pulse for t_y; blue circles $t_y = 9$ μs. (System Ac-d_9/Fl-h_8d_2. $\frac{\omega_{rf}}{2\pi} = 171$ MHz$= \frac{\omega_0}{2\pi}$, $\sqrt{2} \cdot \frac{\omega_{1x}}{2\pi} = \sqrt{2} \cdot \frac{\omega_{1y}}{2\pi} = 12$ MHz, $\frac{\omega_n}{2\pi} = 2.0$ MHz, $T =$ 300 K).